

Higher order zone-folded modes in ZnSe-ZnS strained-layer superlattices

Aishi Yamamoto, Yoshihiko Kanemitsu, and Yasuaki Masumoto
Institute of Physics, University of Tsukuba, Tsukuba, Ibaraki 305, Japan

Shigeki Yamaga and Akihiko Yoshikawa

Department of Electrical and Electronics Engineering, Chiba University, Inage-ku, Chiba 263, Japan

(Received 26 May 1992; accepted for publication 29 July 1992)

Higher order (up to the 5th order) zone-folded acoustic modes in ZnSe-ZnS strained-layer superlattices (SLSs) were observed by means of Raman scattering. Structural characterization of both periodicity of superlattices and roughness of the interface was done by means of transmission electron microscopy (TEM). The Raman spectrum of zone-folded modes was well explained by the theoretical calculation which takes account of two observed structural characteristics of the sample, the periodicity of the superlattices, and the roughness of the interface. This clearly shows the strain does not matter to the observation of the zone-folded modes.

Raman spectroscopy is a very useful tool to study lattice dynamics in semiconductor low-dimensional structures as well as bulk semiconductors. In the case of superlattices, new behavior of phonons, such as zone folding of acoustic phonons and confinement of optical phonons, are studied extensively.¹ The spectra are sensitive to the periodicity, the roughness of the interface, and the stress. Most of II-VI semiconductors superlattices have a biaxial stress at the heterojunction interface due to the lattice mismatch. For example, stress-induced peak shifts of optical phonons were observed in strained-layer superlattices (SLSs).² The spectra of zone-folded acoustic phonons were broad and only the first or second order was observed.^{3,4} One speculates that the lattice mismatch makes it difficult to establish high-quality epitaxial layers and to observe zone-folded modes.

The stress comes from two types of lattice mismatch which exists between SLSs and a substrate, and between the alternate layers in the SLSs. In this work, we were able to observe higher order doublet phonon modes, up to the 5th order, in ZnSe-ZnS SLSs whose average lattice constant⁵ is equal to that of a GaAs substrate. We tried to answer two questions here. One is why such higher order folded modes were observed. The other is whether or not the stress matters to the zone folding of phonon modes. A model calculation based on the transmission electron microscopy (TEM) data was used to consider these problems and it reproduced our zone-folded spectrum. It was found that our Raman spectrum reflects dominantly both the periodicity of the superlattices and the roughness of the interface rather than the stress.

A sample used in this work was ZnSe-ZnS SLSs grown by metalorganic molecular beam epitaxy (MOMBE) on a (100) GaAs substrate.⁵ The designed thickness of ZnSe and ZnS layers were 200 and 10 Å, respectively. The average lattice constant of the SLSs was equal to the GaAs substrate in order to reduce the stress between the SLSs and the substrate. Raman scattering measurements were performed at room temperature with the 4579 Å line of an Ar ion laser in a quasibackscattering configuration. Raman spectrum was obtained by a double monochromator (Spex; 1403) and a photomultiplier.

Figure 1(a) shows the Raman scattering spectrum of zone-folded longitudinal acoustic (LA) modes. The background was subtracted from the spectrum. It is probably originated from Rayleigh scattering and single particle excitations.⁶ Figure 1(a) shows zone-folded doublet modes up to the 5th order. To our knowledge, it is the first observation of such higher order modes in II-VI SLSs. In the continuum limit, a phonon dispersion is given by the conventional Rytov model.⁷ It is written by

$$\cos(qd) = \cos\left(\frac{\omega d_1}{v_1}\right) \cos\left(\frac{\omega d_2}{v_2}\right) - \frac{1+\kappa^2}{2\kappa} \sin\left(\frac{\omega d_1}{v_1}\right) \sin\left(\frac{\omega d_2}{v_2}\right), \quad (1)$$

where ω and q are the phonon frequency and the superlattice wave vector, v_1 and v_2 are the sound velocities of materials 1 and 2, d_1 and d_2 are the thicknesses of the two constituting layers, and d is the period defined by $d = d_1 + d_2$. The coefficient κ is defined by $\kappa = v_1\rho_1/v_2\rho_2$, where ρ_1 and ρ_2 are the corresponding densities. The inset of Fig. 1(a) shows the phonon dispersion calculated by using Eq. (1). We have used $\rho_1 = 5.266 \text{ g/cm}^3$ for ZnSe and $\rho_2 = 4.086 \text{ g/cm}^3$ for ZnS.⁸ The sound velocities used in this calculation were stress-free values in bulk crystals (ZnSe: $v_1 = 4.054 \times 10^5 \text{ cm/s}$, ZnS: $v_2 = 5.047 \times 10^5 \text{ cm/s}$).⁸ The solid circles in the inset are observed peak frequencies of the folded modes. When the thicknesses d_1 and d_2 are designed values 200 and 10 Å, the calculated peak energies do not agree well with the observed ones. The period, d was estimated to be 205 Å from the x-ray diffraction measurement,⁵ though the constituting layer thicknesses, d_1 and d_2 , were not obtained exactly. Therefore, we fixed the period, d , to be 205 Å, and varied the layer thicknesses, d_1 and d_2 , to fit the all of the observed frequencies of the zone-folded modes. The fitted values of d_1 and d_2 were 198 and 7 Å, respectively. These values were used to calculate the dispersion shown in the inset of Fig. 1(a). The calculation fits the experimental data satisfactorily.

So far, zone-folded modes were observed in ZnTe-ZnSe³ and InAs-AlAs⁴ SLSs. It was suggested that the observed peak energies of the folded modes do not com-

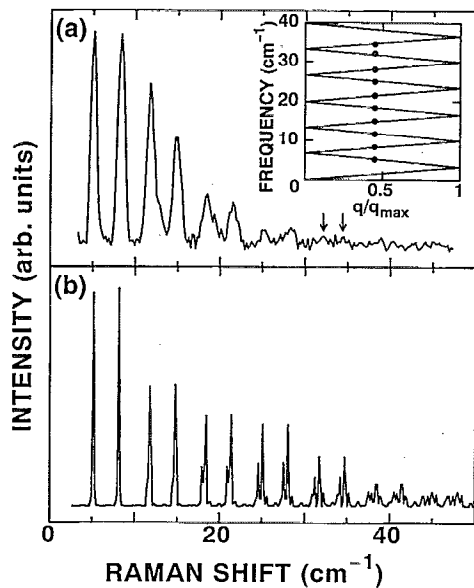


FIG. 1. Observed (a) and calculated (b) Raman spectra of zone-folded modes. The arrows show the peak positions of the fifth-order folded modes. Inset is phonon dispersion using conventional Rytov model, where q_{\max} is the zone-edge wave vector π/d and d is the superlattice period.

pletely agree with the calculated ones. This discrepancy was believed to be originated from the strain between the alternate layers. Recio *et al.*⁴ considered the effect of the strain on the sound velocities deduced from the stress-induced peak shifts of LO-Raman modes and Grüneisen constants. We tried to include the stress effect on the sound velocities using their method. However, all the estimated peak energies were larger than the observed ones by $\sim 0.2 \text{ cm}^{-1}$. The calculation does not fit the experimental data better than the stress-free calculation. Furthermore, it was found that the changing of the thicknesses by a few angstrom induces the peak shift of the folded modes more than the stress.

Figures 2(a) and 2(b) show low- and high-resolution TEM images of our sample, respectively. Figure 2(a) shows good periodicity of each layer. However, a large fluctuation exists near the interface, as shown in Fig. 2(b). Figure 2(c) shows the histogram of the lattice points of ZnS. We obtained each data in the histogram by counting the lattice points of ZnS along the straight arrays of lattice points parallel to the interface plane. The full width at half maximum (FWHM) of the histogram is about four layers and it is a little larger than the fitted values for the thickness of the ZnS layer, 7 \AA . The position at the center of the ZnS layers is fluctuated. Therefore, the FWHM of the histogram is larger than the thickness of the ZnS layer.

The intensity of Raman scattering from the folded LA modes can be theoretically calculated by a photoelastic model, where the superlattices have bulk photoelastic coefficients P_1 and P_2 .⁹ The photoelastic model has been used previously to predict the intensity of the folded modes¹⁰ and to characterize the periodicity and roughness of the interface¹¹ in GaAs-Ga_xAl_{1-x}As superlattices. According to this model, the modulation of the photoelastic coefficient, $P(z)$, along the growth direction z reflects the mod-

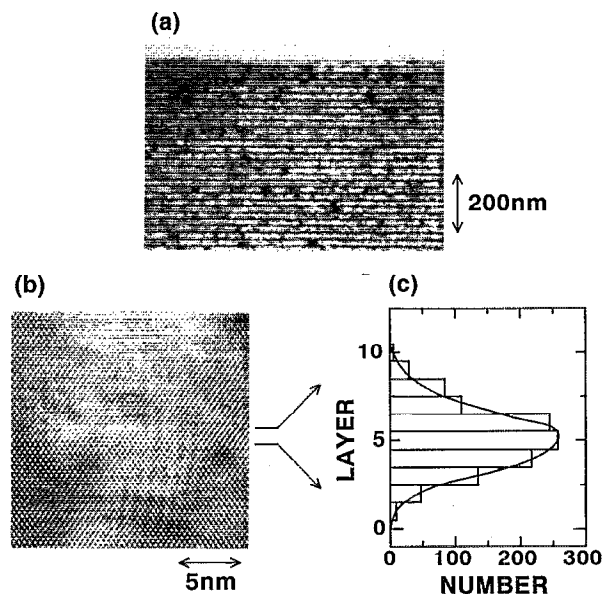


FIG. 2. Low- (a) and high- (b) resolution TEM images. (c) Histogram of the lattice points of ZnS. We obtained the data in the histogram by counting the lattice points of ZnS along the straight arrays of lattice points parallel to the interface plane. The solid line is a guide to the eye.

ulation in the structure of the SLs. The m th order folded modes at $\omega_m = |2m\pi/d \pm q|v_{sl}$ has intensity,

$$I_m \propto \omega_m(n_m + 1) |Q_m|^2, \quad (2)$$

where n_m is the Bose factor, v_{sl} is sound velocity of superlattices defined through $d/v_{sl} = d_1/v_1 + d_2/v_2$, and Q_m is the m th order Fourier component of $P(z)$. It is noted that we do not need the absolute values of P_1 and P_2 , but need only the line shape of $P(z)$ in order to calculate the intensity of Raman spectrum.

When $P(z)$ is assumed to be a square-wave function, in an ideal case, the higher order Fourier component Q_m decreases very slowly. This means that the higher order I_m decreases very slowly. Since the square-wave assumption cannot reproduce our spectrum at all, we took account of the fluctuation of the periodicity and the interface roughness using the TEM data. The roughness of the interface was directly deduced from the distribution of ZnS layers, as shown in Fig. 2(c). The fluctuation of the periodicity, that is the fluctuation of the ZnSe layer thickness, was deduced from two-dimensional densitometric data of the low-resolution TEM image [Fig. 2(a)]. Thus, the profile of $P(z)$ was obtained by taking account of the fluctuation of the periodicity and the roughness of the interface. Figure 3(a) shows the obtained profile of $P(z)$. The intervals between the peaks, that is the fluctuation of the periodicity, are shown in Fig. 3(a). Figure 3(b) shows the Fourier power spectrum, $|Q(k)|^2$ where k is the wave number defined by $k = 2\pi/z$. Several peaks show the m th order Fourier components. The roughness of the interface and the fluctuation of the periodicity cause the decrease of the higher order Q_m . The fluctuation of the periodicity also causes the broadening of the higher order Q_m . By using Eq. (1) and the Fourier components Q_m , the Raman spectrum

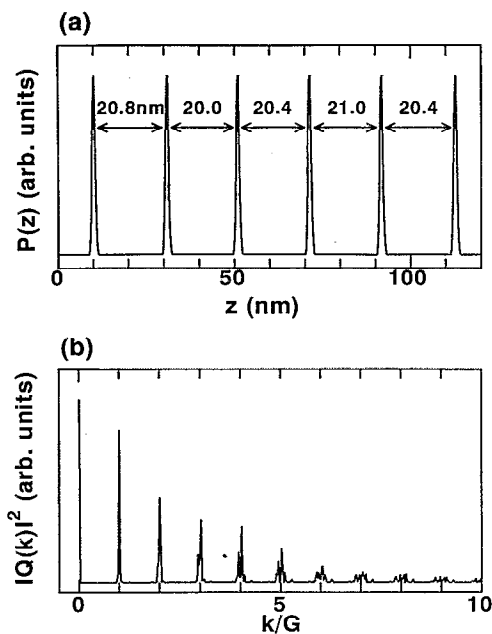


FIG. 3. (a) Photoelastic coefficient $P(z)$ deduced from the TEM images. The intervals between the peak points are shown in the figure, showing the fluctuation of the periodicity. (b) Fourier power spectrum of $P(z)$. G is defined by $G=2\pi/d$, where d is the superlattice period.

of zone-folded modes was calculated, as shown in Fig. 1(b). The Raman spectrum reproduces the experimental data in the following two essential points: the higher order modes become wider and more than 6th order modes reduce their height obviously. In this calculation, we have assumed that the roughness of each layer interface is the same. If the roughness of each layer interface is taken into account, the intensity of the higher order zone-folded modes decreases more and the model calculation reproduces the Raman spectrum more precisely.

In conclusion, we have observed higher order (up to the 5th order) zone-folded acoustic modes in ZnSe-ZnS strained-layer superlattices (SLSs) by means of Raman scattering. We were able to reproduce our zone-folded spectrum using TEM data and a photoelastic model. The agreement between our calculation and the measurement shows that the Raman spectrum reflects dominantly the periodicity of the superlattices and the roughness of the interface.

The authors would like to thank Hitachi Research Laboratory for providing TEM images, and K. Nagao of Fuji Photo Film Co., Ltd. for acquiring two-dimensional densitometric data. Part of this work was done at the Cryogenic Center, University of Tsukuba. This work is partially supported by the Iketani Science and Technology Foundation.

¹ See, for example, *Light Scattering in Solids V*, edited by M. Cardona and G. Güntherodt (Springer, New York, 1989), Vol. 66.

² A. Yamamoto, Y. Yamada, and Y. Masumoto, *Appl. Phys. Lett.* **58**, 2135 (1991).

³ Y. H. Wu, H. Yang, A. Ishida, H. Fujiyasu, S. Nakashima, and K. Tahara, *Appl. Phys. Lett.* **54**, 239 (1989).

⁴ M. Recio, G. Armelles, A. Ruiz, A. Mazuelas, and F. Briones, *Appl. Phys. Lett.* **54**, 804 (1989).

⁵ H. Oniyama, S. Yamaga, and A. Yoshikawa, *Jpn. J. Appl. Phys.* **28**, L2137 (1989).

⁶ M. V. Klein, in *Light Scattering in Solids*, edited by M. Cardona (Springer, New York, 1975), Vol. 8, p. 148.

⁷ S. M. Rytov, *Akust. Zh.* **2**, 71 (1956) [*Sov. Phys. Acoust.* **2**, 68 (1956)].

⁸ Landolt-Börnstein, *Numerical Data and Functional Relationships in Science and Technology* (Semiconductors-Physics of II-VI and I-VII Compounds, Semimagnetic Semiconductors), edited by O. Madelung, M. Schulz, and H. Weiss (Springer, Berlin, 1989), Vol. 17(b), p. 145.

⁹ C. Colvard, T. A. Gant, M. V. Klein, R. Merlin, R. Fischer, H. Morkoç, and A. C. Gossard, *Phys. Rev. B* **31**, 2080 (1985).

¹⁰ M. V. Klein, C. Colvard, R. Fischer, and H. Morkoç, *J. Phys. (Paris) Colloq. C* **5**, C5-131 (1984).

¹¹ S. K. Hark, B. A. Weinstein, and R. D. Burnham, *J. Appl. Phys.* **62**, 1112 (1987).